Behavioral/Systems/Cognitive

Functional Asymmetry for Auditory Processing in Human Primary Auditory Cortex

Joseph T. Devlin,[1] Josephine Raley,[1] Elizabeth Tunbridge,[1] Katherine Lanary,[1] Anna Floyer-Lea,[1] Charvy Narain,[1] Ian Cohen,[1] Timothy Behrens,[1] Peter Jezzard,[1] Paul M. Matthews,[1] and David R. Moore[2]

[1]Centre for Functional Magnetic Resonance Imaging of the Brain, Department of Clinical Neurology, University of Oxford, John Radcliffe Hospital, Oxford OX3 9DU, United Kingdom, and [2]Medical Research Council Institute of Hearing Research, University Park, Nottingham NG7 2RD, United Kingdom

Structural asymmetries in the supratemporal plane of the human brain are often cited as the anatomical basis for the lateralization of language predominantly to the left hemisphere. However, similar asymmetries are found for structures mediating earlier events in the auditory processing stream, suggesting that functional lateralization may occur even at the level of primary auditory cortex. We tested this hypothesis using functional magnetic resonance imaging to evaluate human auditory cortex responses to monaurally presented tones. Relative to silence, tones presented separately to either ear produced greater activation in left than right Heschl's gyrus, the location of primary auditory cortex. This functional lateralization for primary auditory cortex is distinct from the contralateral dominance reported for other mammals, including nonhuman primates, and may have contributed to the evolution of a unique role for the left hemisphere in language processing.

Key words: auditory; lateralization; hemisphere; imaging; sensory neurons; speech

Introduction

The human ability to understand spoken language is mostly dependent on a left lateralized cortical system (Binder et al., 2000; Price, 2000; Scott et al., 2000), and this functional lateralization has been associated with structural asymmetries in the supratemporal plane (Geschwind and Galaburda, 1985; Foundas et al., 1994). Both the primary auditory cortex (PAC) and the adjacent nonprimary regions are typically larger in the left hemisphere than the right (Geschwind and Levitsky, 1968; Galaburda et al., 1978; Rademacher et al., 1993; Penhune et al., 1996; Shapleske et al., 1999), and these gross anatomical differences are also mirrored at the microstructure level (Anderson et al., 1999; Galuske et al., 2000; Buxhoeveden et al., 2001). Because these regions are not selective for processing speech, humans may exhibit a left hemisphere dominance for auditory processing. This would distinguish human sound processing from that of most animals, for which both behavioral and electrophysiological studies have demonstrated a functional contralateral dominance in the PAC (Brugge and Merzenich, 1973; Reale and Kettner, 1986; Clarey et al., 1992; Rutkowski et al., 2000). Although previous work has suggested that humans also exhibit a contralateral dominance for cortical auditory processing (Pantev et al., 1998; Scheffler et al., 1998; Woldorff et al., 1999; Jancke et al., 2002), methodological

limitations did not allow these studies to distinguish clearly between PAC and nonprimary auditory cortical responses. Thus, they are difficult to directly compare with the animal literature. Here, we distinguish between these competing hypotheses regarding the lateralization of brain activity in human PAC using functional magnetic resonance imaging (fMRI) with an anatomical segmentation that has allowed us to distinguish activity in primary and nonprimary areas separately.

Materials and Methods

The acoustic noise associated with echo–planar imaging [which can exceed a 110 dB sound pressure level (SPL) in a 3 Tesla magnetic field] is a serious confound for fMRI studies of auditory processing. Here, we used a "sparse sampling" (Hall et al., 1999) protocol to measure cortical auditory responses in primary and surrounding nonprimary auditory cortices to monaurally presented tones. This technique separates responses to the stimuli from those caused by the (binaural) noise of the MRI scanner by taking advantage of the hemodynamic lag in the blood oxygenation level-dependent (BOLD) signal and the fact that the signal decays to within 10% of its resting level within 7 sec of the offset of scanning, ensuring that each trial is unaffected by previous ones (Fig. 1). Participants were asked to discriminate between high (4000 Hz) and low (250 Hz) frequency tones by pressing one of two buttons as quickly as possible after the tone onset. An equal number of silent trials were included in which no tone was played and no response was required. The purpose of the task was simply to control attention by forcing subjects to attend to the tones throughout the scan.

Twelve adults (four females and eight males) with normal hearing (pure tone average, ≤20 dB hearing loss) participated in this experiment. Their ages ranged from 20 to 30 years (mean, 24), and all were strongly right handed, as assessed with the Edinburgh handedness inventory (Oldfield, 1971). None had a personal or family history of any neurological disease, and each gave informed consent after the experimental
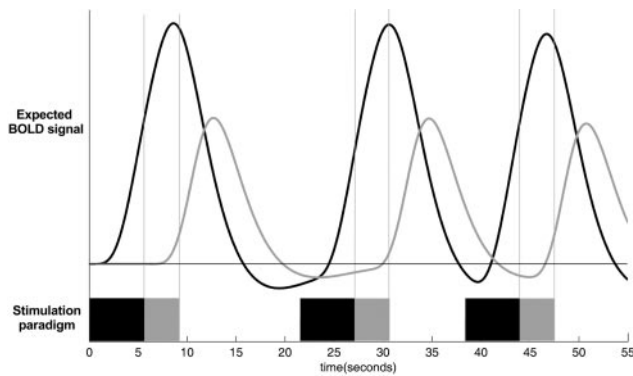
Figure 1. Sparse sampling protocol. The bottom portion of the graph shows the stimulation paradigm with auditory tone or silence stimuli (black) presented for 6 sec, followed immediately by a 3 sec whole brain volume acquisition (gray). Each trial was followed by a variable length intertrial interval ranging from 7 to 14 sec. The top portion of the graph shows the expected BOLD response to both the tones (black) and the noise (gray) of the scanner. The vertical lines indicate that the sampled BOLD response was at or near its peak levels from the tone stimulation. In addition, the intertrial interval was sufficiently long to allow the auditory response to return to within 10% of its resting level, so that each trial was unaffected by previous ones.

methodology was explained. The experiment was approved by the Central Oxford Research Ethics Committee.

The tone stimuli consisted of a 5 Hz sinusoidal amplitude-modulated tone with a carrier frequency of 250 or 4000 Hz and total duration of 6 sec. This rate of presentation was found to be optimal for activating PAC (Giraud et al., 2000; Tanaka et al., 2000; Hall et al., 2002; Harms and Melcher, 2002). Tones were presented monaurally at a 90 dB SPL in a pseudorandomized manner using the Medical Research Council Institute of Hearing Research MR sound system (Palmer et al., 1998) with MR compatible electrostatic headphones (Sennheiser model HE 60) and modified industrial ear protectors (Bilsom model 2452). Interaural cross-talk for these headphones has been measured at −31 and less than −60 dB, for 250 and 4000 Hz stimuli, respectively. Because low level (<50 dB SPL) tones do not produce any measurable activation (our unpublished data), it is unlikely that cross-talk would have contributed significantly to observed brain responses. Sound level calibration was performed separately for each headphone using a Brüel and Kjær measuring amplifier (model 2610) and associated preamplifier (model 2619), microphone (model 4134), and artificial ear (model 4153).

All subjects participated in two scanning runs. Tones within one run were presented to the left ear, and those within the other were presented to the right ear, fully counterbalanced across participants. Within each run, stimuli were pseudo-randomized in an event-related presentation. A trial began with 6 sec of stimulation (i.e., a high or low frequency tone or a silent trial), during which the gradient coil was turned off, followed immediately by 3 sec of acquisition (one brain volume). Subjects were asked to press a button to indicate whether the tone was high or low frequency. Intertrial intervals varied between 7 and 14 sec to minimize anticipation of the upcoming trial. Consequently, the full time between successive volume acquisitions varied between 16 and 23 sec (Fig. 1).

Scanning was performed using the Varian-Inova 3T scanner at the Centre for Functional Magnetic Resonance Imaging of the Brain (FMRIB) in Oxford, United Kingdom. A Magnex head-dedicated gradient insert coil was used in conjunction with a birdcage head radiofrequency coil tuned to 127.4 MHz. Functional imaging consisted of 21 T2*-weighted echo–planar image (EPI) slices [echo time (TE), 30 msec; field of view, 192 × 256 mm; matrix, 64 × 64], giving a notional 3 × 4 × 5 mm resolution. An automated shimming algorithm was used to reduce magnetic field inhomogeneities (Wilson et al., 2002). To define Heschl's gyrus (HG) in each subject, a T1-weighted scan was acquired (three-dimensional Turbo fast, low angle shot sequence; repetition time, 15 msec; TE, 6.9 msec) with 1 mm² in-plane resolution and either 1.5 mm or 3 mm slice thickness.

The functional images were realigned (Jenkinson et al., 2002) to cor-

rect for small head movements using the FMRIB Software Library (FSL) software (http://www.fmrib.ox.ac.uk/fsl). Functional images were registered to the participant's structural scan and then to the Montreal Neurological Institute 152-mean brain using an affine procedure (Jenkinson and Smith, 2001). Finally, each image was smoothed with a 5 mm (at full-width half-maximum) Gaussian filter. The FSL software was used to compute individual subject analyses using the general linear model (Woolrich et al., 2001). Tone trials (high and low) were modeled as a single factor of interest, and the estimated motion parameters for each subject were included as covariates of no interest to reduce spurious activations because of head motion, thereby increasing statistical sensitivity. Random effects group analyses identified significantly activated brain regions. A cluster-based significance test was used with a height threshold of $Z > 3.5$ and $p < 0.05$, corrected for multiple comparisons (Friston et al., 1994). Results are reported specifically for auditory areas, namely primary and nonprimary auditory cortices and the medial geniculate nucleus (MGN) of the thalamus.

To evaluate hemispheric asymmetries within auditory areas, we computed laterality indices (LI) based on two separate measures of activity in the selected regions of interest (ROI) for each participant:

$$ \text{LI} = \frac{\text{contralateral BOLD signal} - \text{ipsilateral BOLD signal}}{\text{contralateral BOLD signal} + \text{ipsilateral BOLD signal}} \times 100 $$

LI values ranged from +100, indicating completely contralateral activation, to −100, indicating completely ipsilateral activation. Equal activations contralateral and ipsilateral to the stimulated ear produced a value of 0. BOLD signal was measured as either (1) the mean percentage BOLD signal change or (2) the volume of "active" tissue normalized to the volume of the ROI. Both measures are insensitive to differences in the volume or location of the ROI across hemispheres. Even so, the latter measure can potentially bias the laterality calculation by introducing an arbitrary threshold for excluding voxels. If the results of the analysis remain similar over a range of thresholds, however, the validity of the calculation is maintained. Consequently, voxels were defined as active over a range of thresholds ($Z > 2.3, 3.1, 3.5,$ and 4.0) for all laterality calculations. Separate analyses were conducted for the three ROI, namely the primary and nonprimary auditory cortices as well as the MGN. These regions were identified according to anatomical and functional criteria.

The majority of PAC is located on HG despite some individual variation in the precise cytoarchitectonic borders of the region (Rademacher et al., 1993, 2001; Penhune et al., 1996; Hackett et al., 2001; Morosan et al., 2001). Thus, for each participant, the first transverse temporal gyrus was labeled in both hemispheres using three-dimensional visualization software (http://www.psychology.nottingham.ac.uk/staff/cr1/mricro.html). The gyrus was bordered anteromedially by the first transverse sulcus and posterolaterally by Heschl's sulcus, except in four participants in whom HG was either duplicated or partially duplicated. In these cases, only the region anterior to the second transverse sulcus was labeled, following Rademacher et al. (1993). Patterson et al. (2002) have recently shown an excellent correspondence between this anatomical measure of HG and estimates of PAC from cytoarchitecture. For each label, the center of gravity (COG) was computed and transformed into standard space. The mean COG was x = −41, y = −26, and z = +6 in the left hemisphere and x = +47, y = −22, and z = +7 in the right hemisphere, with a significant anterior shift for right HG (paired t test; $t_{(11)} = -3.8$; $p < 0.01$) as seen in previous studies (Rademacher et al., 1993, 2001; Penhune et al., 1996; Patterson et al., 2002).

Unlike PAC, the precise borders of the nonprimary auditory regions are unclear from structural landmarks on the anatomical images (Rivier and Clarke, 1997). Consequently, we identified the non-PAC ROI functionally, rather than anatomically, based on the results of the group functional activation maps. Voxels activated ($Z > 3.5$) by tones relative to silence were masked to include only those within the auditory regions of the supratemporal plane and insular cortex (x = ±36–76, y = +4 to −22, and z = −6 to + 22), coordinates chosen to conservatively encompass the nonprimary auditory regions identified by Rivier and Clark (1997). Nonauditory regions included in the mask would not be expected to be activated by auditory stimulation and, therefore, would not be

included in the ROI. For each subject, HG was removed from the non-primary ROI to exclude the PAC. Note that by defining nonprimary regions in terms of active voxels, it becomes necessary to again use a range of thresholds to confirm relative laterality.

Finally, because the primary and nonprimary auditory fields receive direct projections from the MGN, relative activation was assessed in an ROI defined to include this nucleus. Individual thalamic nuclei are not, however, distinguishable on T1-weighted MRI images; consequently, MGN was identified based on published standard space coordinates from cytoarchitectonic and myeloarchitectonic studies (Niemann et al., 2000) and from the characteristic fiber orientations of the corticothalamic striations identified *in vivo* using diffusion tensor imaging (DTI) (Wiegell et al., 2003). The ROI was defined as x = ±10–20, y = −12 to −20, and z = 0 to −6. Thus, MGN was defined anatomically, although the accuracy of the definition for individual brains depends on the accuracy of their registration to the standard brain space.

Results

Performance was nearly perfect for left (L) and right (R) ear stimulation with no differences in either accuracy (mean ± SEM: L, 97 ± 2%; R, 98 ± 1%; $t_{(11)} = 1.6$; NS) or reaction times (L, 1025 ± 69 msec; R, 1073 ± 71 msec; $t_{(11)} = 0.3$; NS). For both left and right ear stimulation, monaurally presented tones led to bilateral activity in PAC and nonprimary areas surrounding HG, including the anterior auditory region of insular cortex. This is illustrated for a single subject in Figure 2, in which the activation is displayed on an "inflated brain" (Fischl et al., 1999) to facilitate visualization of supratemporal structures within the Sylvian fissure. In addition, there was bilateral activity present in the MGN of the thalamus (Table 1).

Within PAC, monaurally presented tones led to greater activity in the left hemisphere, regardless of which ear was stimulated. When the LI were based on mean percentage BOLD signal change, left ear stimulation led to a clear ipsilateral advantage (mean LI = −20 ± 6; $t_{(11)} = -3.39$; $p < 0.01$) (Fig. 3a), with greater left than right hemisphere activity in 10 of 12 subjects, whereas right ear stimulation produced significantly greater contralateral activation (LI = 59 ± 8; $t_{(11)} = 7.0$; $p < 0.001$) in 12 of 12 subjects. The same pattern was observed when the volume of active tissue was considered instead: left ear stimulation led to a small, but significant, ipsilateral advantage (mean LI = −8 ± 2; $t_{(11)} = -3.64$; $p < 0.01$), with greater left than right hemisphere activity in 10 of 12 subjects, whereas right ear stimulation produced significantly greater contralateral activation (LI = 18 ± 4; $t_{(11)} = 5.45$; $p < 0.001$) in 11 of 12 subjects. The presence of this asymmetry was independent of the statistical threshold used to define active voxels (Table 2). In other words, it was important to demonstrate that the specific statistical threshold used to classify voxels as active did not substantially alter the pattern of results. Across a range of thresholds, the results of the laterality calculations in PAC remained the same, demonstrating a reliable left hemisphere advantage.

In contrast, within nonprimary areas, auditory stimulation of either ear led to a small contralateral advantage. Left ear stimulation yielded a mean LI of 7 ± 3 ($t_{(11)} = 2.0$; $p < 0.07$), with 8 of 12 participants showing a small contralateral lateralization. Similarly, right ear stimulation produced significantly greater contralateral activation across subjects (mean LI = 9 ± 3; $t_{(11)} = 2.1$; $p < 0.05$) (Fig. 3b). This asymmetry was found in 11 of 12 subjects. Because the definition of the nonprimary ROI relied, in part, on an arbitrarily chosen statistical threshold (i.e., Z > 3.5 for active voxels in the group analysis), it was important to demonstrate that the specific threshold did not substantially alter the pattern of results. Across a range of thresholds, the results of the
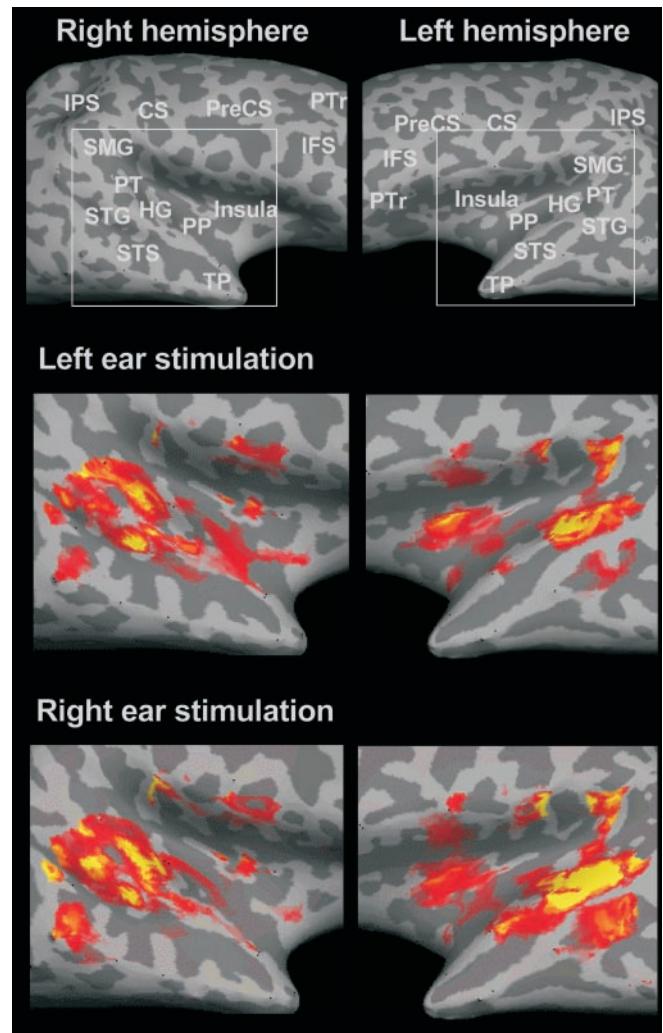

Figure 2. Auditory cortex activations for monaural tones relative to silence for a single participant. The top panels display lateral views of the inflated left and right hemisphere surfaces with sulci and gyri shown in dark and light gray, respectively (Fischl et al., 1999). The middle and bottom panels show activation in cortical auditory fields attributable to left and right ear stimulation. CS, Central sulcus; IFS, inferior frontal sulcus; IPS, intraparietal sulcus; PP, planum polare; PT, planum temporale; PreCS, precentral sulcus; PTr, pars triangularis; SMG, supramarginal gyrus; STG, superior temporal gyrus; STS, superior temporal sulcus; TP, temporal pole.

laterality calculations in nonprimary areas remained qualitatively and quantitatively similar, although the statistical reliability of the laterality effect varied (Table 3).

LI were also calculated for the MGN, in which there was no significant lateralization of responses for either left (LI = −2 ± 11; $t_{(11)} = -0.4$; NS) or right (LI = 14 ± 7; $t_{(11)} = 1.1$; NS) ear stimulation when based on mean percentage BOLD signal change (Fig. 4). Measurements based on active tissue volume gave similar results, except at the most lenient statistical threshold in which there was a significant contralateral dominance for right (LI = 35 ± 12; $t_{(10)} = 2.7$; $p < 0.05$) but not left (LI = −4 ± 19; $t_{(9)} = -0.9$; NS) ear stimulation. In this respect, the results mirrored the stronger contralateral activation in the PAC produced by right ear stimulation (Fig. 3). Note, however, that several participants had no active voxels in either the right or left ROI, even at statistical thresholds as low as Z > 2.3 ($p = 0.01$; uncorrected), possibly because of its very small size (240 mm³) and the relatively low resolution of the EPI sequence (3 × 4 × 5 mm) (Table 4).

Table 1. Group activations for monaural pure tone stimulation relative to silence in cortical and subcortical auditory areas

Description[a]	Left ear stimulation				Right ear stimulation			
	x	y	z	Z_{peak}	x	y	z	Z_{peak}
L. PAC	−46	−22	4	4.2	−46	−24	4	4.3
R. PAC	46	−18	2	4.2	44	−26	8	3.9
Nonprimary areas								
L. PA	−38	−32	8	4.7	−42	−30	8	4.8
R. PA	46	−30	8	5.2	50	−30	8	5.3
L. LA	−52	−30	10	5.1	−62	−28	8	3.7
R. LA	60	−24	6	4.7	62	22	10	3.7
L. MA	−38	−20	6	3.7	−40	−20	−2	4.2
R. MA	48	−14	−2	5.6	44	−18	0	3.7
L. STA	−64	−22	2	3.7	−62	−22	0	4.2
R. STA	64	−28	8	4.6	66	−28	12	4.7
L. AIA	−38	−6	4	4.6	−38	0	2	5.2
R. AIA	38	−4	2	3.7	36	2	6	4.2
Auditory thalamus								
L. MG	−16	−18	0	3.9	−12	−12	−2	5.0
R. MG	12	−16	0	3.5	12	−16	0	3.8

[a]The location of the auditory fields was estimated from the probabilistic PAC atlas of Rademacher et al. (2001) and the standard space coordinates of nonprimary regions identified by Rivier and Clarke (1997). L., Left; R., right; PA, posterior area; MA, medial area; LA, lateral area; STA, superior temporal area; AIA, anterior insula area.
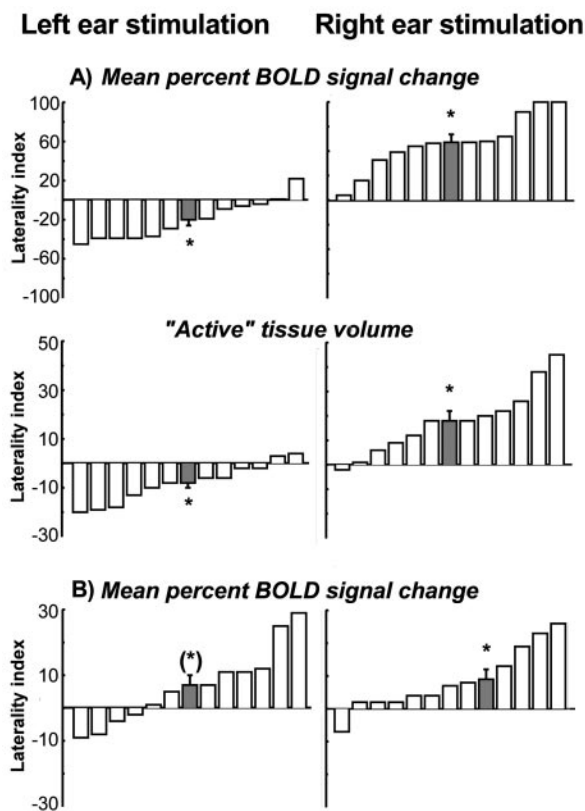

Figure 3. LI for individuals (white) and the group mean ± SEM (gray) for PAC localized to HG (a) and adjacent non-PAC defined according to functional and anatomical criteria (b). In PAC, monaural tones to both the left and right ear produced a highly significant left hemisphere advantage, regardless of whether responses were based on mean percentage BOLD signal change (top row) or the volume of active tissue (middle row; voxels were considered active at $Z > 3.5$). In non-PAC, monaural auditory stimulation was associated with greater contralateral activity, although this was only a trend for left ear stimulation. Active tissue volumes are not present for the nonprimary area because the definition of active was the same as the definition of the ROI, thereby yielding a constant volume of 1.0.

Table 2. LI in PAC for left and right ear stimulation based on normalized volume of active tissue

Threshold	LI*	
	Left ear stimulation	Right ear stimulation
$Z > 4.0$	−8 ± 2	18 ± 4
$Z > 3.5$	−8 ± 2	18 ± 4
$Z > 3.1$	−8 ± 2	17 ± 4
$Z > 2.3$	−8 ± 2	17 ± 4

*$p < 0.01$, based on a paired sample t test of volume of active tissue within left and right PAC across individual participants (df = 11).

Table 3. LI in nonprimary regions for left and right ear stimulation

Masking threshold	LI	
	Left ear stimulation	Right ear stimulation
$Z > 4.0$	8 ± 3**	4 ± 3
$Z > 3.5$	7 ± 3***	9 ± 3*
$Z > 3.1$	6 ± 3	10 ± 3*
$Z > 2.3$	7 ± 4	11 ± 5**

The statistical threshold was used to identify the set of voxels "activated" by tones versus silence in the group random effect analysis. This mask was then limited to supratemporal auditory regions and adjusted to removed HG per participant. Within the resulting mask, the LI are based on the mean percentage BOLD signal change.

*$p < 0.01$, **$p < 0.05$, ***$p < 0.1$, based on a paired sample t test of mean percentage BOLD signal change in the left and right nonprimary areas across individual participants (df = 11).

contralateral advantage in the adjacent nonprimary regions and no clear lateralization in the auditory thalamus. Although the current study is the first to separate primary from nonprimary responses, future work possibly with high-resolution fMRI and novel locator paradigms will be necessary to evaluate the laterality of the individual nonprimary regions. Similarly, a combination of DTI and high-resolution fMRI should make it possible to unambiguously locate MGN in individuals according to its characteristic fiber orientations (Wiegell et al., 2003) and to reliably assess its laterality. The strength of the current study, however, is a clear and robust left hemisphere dominance in PAC.

In contrast to the current results, previous magnetoencephalography and fMRI studies have reported a contralateral dominance for monaural auditory processing (Pantev et al., 1998; Scheffler et al., 1998; Woldorff et al., 1999; Jancke et al., 2002), although none have distinguished between the dominance in primary and nonprimary regions. In fact, auditory-evoked fields (AEFs) exhibit complex spatiotemporal patterns, making it im-
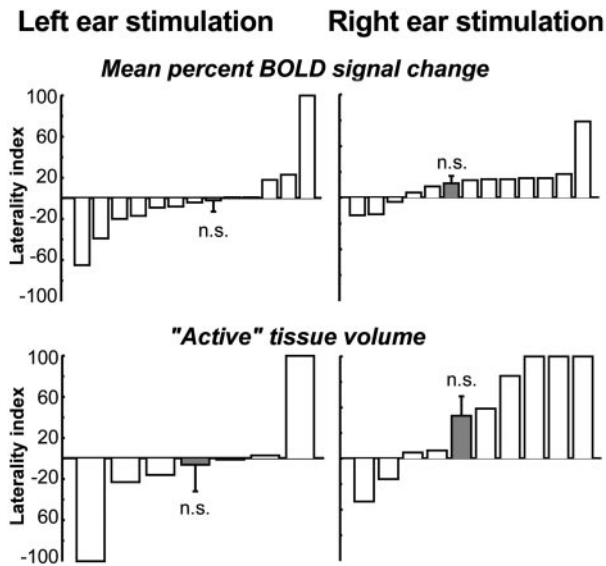
Discussion

Here, we have demonstrated a clear left hemisphere dominance for processing tones in human PAC that contrasts with a weak

Figure 4. LI for individuals (white) and the group mean ± SEM (gray) for the MGN. Monaurally presented tones did not produce a clear pattern of lateralization. When responses were based on mean percentage BOLD signal change (top row), there was no significant difference between ipsilateral and contralateral responses. The same was true when responses were based on the volume of active tissue, but note that only a subset of participants had any active voxels in either the left or right ROI at $Z > 3.5$.

Table 4. LI for the MGN based on the two measures of brain activity, mean percentage BOLD signal change and normalized volume of active tissue

Threshold	MGN	
	Left ear (n)	Right ear (n)
Mean percentage BOLD signal change		
Not applicable	−2 ± 11	14 ± 7
Normalized volume of active tissue		
$Z > 4.0$	−9 ± 27 (6)	9 ± 28 (7)
$Z > 3.5$	−6 ± 26 (6)	42 ± 19 (9)
$Z > 3.1$	−18 ± 21 (9)	37 ± 15 (9)
$Z > 2.3$	−4 ± 19 (10)	35 ± 12* (11)

The statistical threshold used to identify active voxels ranged from 4.0 to 2.3. *n* refers to the number of participants (of 12) who had active voxels in either the left or right (or both) ROI.

*$p < 0.05$. *p* values are based on paired sample *t* tests of measured activation within left and right MGN across individual participants (df = n − 1).

possible to identify a component of the AEF that is specific to PAC (Lutkenhoner et al., 2003). Thus, the two studies (Pantev et al., 1998; Woldorff et al., 1999) showing a contralateral dominance based on lateralization of the N1m component were most likely reflecting responses in nonprimary regions lateral to PAC (Liegeois-Chauvel et al., 1994; Pantev et al., 1995), consistent with our results. Previous fMRI studies (Scheffler et al., 1998; Woldorff et al., 1999; Jancke et al., 2002; Suzuki et al., 2002) also have not distinguished between cortical auditory fields. When primary and nonprimary regions were combined for lateralization analysis using results from the current study, a small contralateral advantage also emerged. This predominantly reflects the small contralateral advantage of the larger volume of non-PAC. In addition, a potential confound of previous fMRI studies is that they used "blocked" designs in which auditory stimuli (and silence) were masked by the loud binaural, spectrally complex noise of the scanner. It is well known that nonprimary regions respond more strongly to complex sounds than to tones (Wessinger et al., 2001) and, thus, may further mask the response of PAC. If subjects focused their attention on the side of stimulation while actively suppressing sounds from the other ear (i.e., scanner

noise) in compensation, then spatial attention may have introduced an additional contralateral bias further affecting the laterality of processing. The current study used a sparse sampling protocol with an event-related design and controlled attention to provide a more sensitive measure of auditory processing, greater anatomical precision, and a better-defined cognitive state.

Our study involved discrimination between two fixed tones. Other studies have suggested that processing spectral information, such as pitch, preferentially relies on the right hemisphere (Zatorre et al., 2002). For example, dichotic listening (Cohen et al., 1989), functional neuroimaging (Zatorre et al., 1992; Belin et al., 1998), and lesion studies (Peretz, 1990; Robin et al., 1990) all found a right hemisphere advantage for processing pitch (for review, see Wong, 2002). A crucial aspect of these studies, however, is that the advantage was found for stimuli with dynamic pitch variation (e.g., melodies) rather than for pitch *per se*. The hemispheric asymmetry occurred in regions of the superior temporal gyrus and planum polare anterior to PAC (Patterson et al., 2002). Thus, the results of the current study complement, rather than conflict with, this right hemispheric advantage for pitch processing.

Our results demonstrate that within PAC there is a left hemisphere dominance for processing simple auditory stimuli. If speech-specific operations do not begin until the signal reaches the cerebral cortex (Scott and Johnsrude, 2003), then one function of PAC may be to determine whether an incoming signal has sufficient spectral and temporal complexity to be treated as speech. A left hemisphere advantage would then facilitate the rapid temporal processing in adjacent left hemisphere auditory areas (Zatorre et al., 2002). If correct, this may explain why this pattern of functional organization is different from the contralateral dominance seen in other species, including other primates (Brugge and Merzenich, 1973; Clarey et al., 1992). In contrast, like humans, at least two species of great apes, chimpanzees (*Pan troglodyte*) and gorillas (*Gorilla gorilla*), show structural auditory cortex asymmetries that are not seen in macaques (*Macaca mulatto*) (Yeni-Komshian and Benson, 1976; Gannon et al., 1998; Hopkins et al., 1998). Thus, there seems to be a hierarchy in the degree of hemispheric lateralization in primates, with monkeys showing the least asymmetry and humans the most. Whether the relative difference in structural asymmetry is matched by a corresponding functional shift from a contralateral auditory dominance to a left hemisphere dominance in chimpanzees and gorillas, or whether left functional lateralization for auditory processing is unique to humans, remains to be demonstrated.

These observations have two important implications. First, they suggest the possibility that evolution of audition helped to drive the specialization in the left hemisphere for language. Approximately 90% of normal, right-handed speakers show a left hemisphere dominance for language (Springer et al., 1999), similar to the left hemisphere dominance reported here. This argues for the primacy of hearing in the evolution of language and, hence, for a "bottom-up" evolution, as opposed to a "top-down," linguistic-based evolution. Second, these results call into question the appropriateness of using the macaque auditory system as a model for human auditory organization. In a recent study, Poremba et al. (2003) measured glucose use in awake rhesus monkeys passively listening to auditory stimuli to identify the full extent of the macaque auditory system that included not only the full superior temporal gyrus but also extensive parietal, prefrontal, and limbic cortices. They concluded that their results "help close the gap between the human and monkey cerebral auditory systems in terms of both their extent and organization" (p. 572).

We think our results widen that gap and challenge inferences based on presumed similarities between cortical auditory processing in monkeys and man.

References

Anderson B, Southern BD, Powers RE (1999) Anatomic asymmetries of the posterior superior temporal lobes: a postmortem study. Neuropsychiatry Neuropsychol Behav Neurol 12:247–254.

Belin P, Zilbovicius M, Crozier S, Thivard L, Fontaine A, Masure MC, Samson Y (1998) Lateralization of speech and auditory temporal processing. J Cognit Neurosci 10:536–540.

Binder JR, Frost JA, Hammeke TA, Bellgowan PS, Springer JA, Kaufman JN, Possing ET (2000) Human temporal lobe activation by speech and non-speech sounds. Cereb Cortex 10:512–528.

Brugge JF, Merzenich MM (1973) Responses of neurons in auditory cortex of the macaque monkey to monaural and binaural stimulation. J Neurophysiol 36:1138–1158.

Buxhoeveden DP, Switala AE, Litaker M, Roy E, Casanova MF (2001) Lateralization of minicolumns in human planum temporale is absent in nonhuman primate cortex. Brain Behav Evol 57:349–358.

Clarey JC, Barone P, Imig TJ (1992) Physiology of the thalamus and cortex. In: The mammalian auditory pathway: neurophysiology (Popper AN, Fay RR, eds), pp 232–334. New York: Springer.

Cohen H, Levy JJ, McShane D (1989) Hemispheric specialization for speech and non-verbal stimuli in Chinese and French Canadian subjects. Neuropsychologia 27:241–245.

Fischl B, Sereno MI, Dale AM (1999) Cortical surface-based analysis. II: Inflation, flattening, and a surface-based coordinate system. NeuroImage 9:195–207.

Foundas AL, Leonard CM, Gilmore R, Fennell E, Heilman KM (1994) Planum temporale asymmetry and language dominance. Neuropsychologia 32:1225–1231.

Friston KJ, Worsley KJ, Frackowiak RSJ, Mazziotta JC, Evans AC (1994) Assessing the significance of focal activations using their spatial extent. Hum Brain Mapp 1:214–220.

Galaburda AM, Sanides F, Geschwind N (1978) Human brain. Cytoarchitectonic left-right asymmetries in the temporal speech region. Arch Neurol 35:812–817.

Galuske RA, Schlote W, Bratzke H, Singer W (2000) Interhemispheric asymmetries of the modular structure in human temporal cortex. Science 289:1946–1949.

Gannon PJ, Holloway RL, Broadfield DC, Braun AR (1998) Asymmetry of chimpanzee planum temporale: humanlike pattern of Wernicke's brain language area homolog. Science 279:220–222.

Geschwind N, Galaburda AM (1985) Cerebral lateralization. Biological mechanisms, associations, and pathology: III. A hypothesis and a program for research. Arch Neurol 42:634–654.

Geschwind N, Levitsky W (1968) Human brain: left-right assymetries in temporal speech region. Science 161:186–187.

Giraud A-L, Lorenz C, Ashburner J, Wable J, Johnsrude I, Frackowiak R, Kleinschmidt A (2000) Representation of the temporal envelope of sounds in the human brain. J Neurophysiol 84:1588–1598.

Hackett TA, Preuss TM, Kaas JH (2001) Architectonic identification of the core region in auditory cortex of macaques, chimpanzees, and humans. J Comp Neurol 441:197–222.

Hall DA, Haggard MP, Akeroyd MA, Palmer AR, Summerfield AQ, Elliot MR, Gurney EM, Bowtell RW (1999) "Sparse" temporal sampling in auditory fMRI. Hum Brain Mapp 7:213–223.

Hall DA, Johnsrude IS, Haggard MP, Palmer AR, Akeroyd MA, Summerfield AQ (2002) Spectral and temporal processing in human auditory cortex. Cereb Cortex 12:140–149.

Harms MP, Melcher JR (2002) Sound repetition rate in the human auditory pathway: representations in the waveshape and amplitude of fMRI activation. J Neurophysiol 88:1433–1450.

Hopkins WD, Marino L, Rilling JK, MacGregor LA (1998) Planum temporale asymmetries in great apes as revealed by magnetic resonance imaging (MRI). NeuroReport 9:2913–2918.

Jancke L, Wustenberg T, Schulze K, Heinze HJ (2002) Asymmetric hemodynamic responses of the human auditory cortex to monaural and binaural stimulation. Hear Res 170:166–178.

Jenkinson M, Smith SM (2001) A global optimisation method for robust affine registration of brain images. Med Image Anal 5:143–156.

Jenkinson M, Bannister P, Brady M, Smith S (2002) Improved optimization for the robust and accurate linear registration and motion correction of brain images. NeuroImage 17:825–841.

Liegeois-Chauvel C, Musolino A, Badier JM, Marquis P, Chauvel P (1994) Evoked potentials recorded from the auditory cortex in man: evaluation and topography of the middle latency components. Electroencephalogr Clin Neurophysiol 92:204–214.

Lutkenhoner B, Krumbholz K, Lammertmann C, Seither-Preisler A, Steinstrater O, Patterson RD (2003) Localization of primary auditory cortex in humans by magnetoencephalography. NeuroImage 18:58–66.

Morosan P, Rademacher J, Schleicher A, Amunts K, Schormann T, Zilles K (2001) Human primary auditory cortex: cytoarchitectonic subdivisions and mapping into a spatial reference system. NeuroImage 13:684–701.

Niemann K, Mennicken VR, Jeanmonod D, Morel A (2000) The morel stereotactic atlas of the human thalamus: atlas-to-MR registration of internally consistent canonical model. NeuroImage 12:601–616.

Oldfield RC (1971) The assessment and analysis of handedness: the Edinburgh inventory. Neuropsychologia 9:97–113.

Palmer AR, Bullock DC, Chambers JD (1998) A high-output, high quality sound system for use in auditory fMRI. NeuroImage 7:S359.

Pantev C, Bertrand O, Eulitz C, Verkindt C, Hampson S, Schuierer G, Elbert T (1995) Specific tonotopic organizations of different areas of the human auditory cortex revealed by simultaneous magnetic and electric recordings. Electroencephalogr Clin Neurophysiol 94:26–40.

Pantev C, Ross B, Berg P, Elbert T, Rockstroh B (1998) Study of the human auditory cortices using a whole head magnetometer: left vs. right hemisphere and ipsilateral vs. contralateral stimulation. Audiol Neurootol 3:183–190.

Patterson RD, Uppenkamp S, Johnsrude IS, Griffiths TD (2002) The processing of temporal pitch and melody information in auditory cortex. Neuron 36:767–776.

Penhune VB, Zatorre RJ, Macdonald JD, Evans AC (1996) Interhemispheric anatomical differences in human primary auditory cortex: probabilistic mapping and volume measurement from magnetic resonance scans. Cereb Cortex 6:661–672.

Peretz I (1990) Processing of local and global musical information by unilateral brain-damaged patients. Brain 113:1185–1205.

Poremba A, Saunders RC, Crane AM, Cook M, Sokoloff L, Mishkin M (2003) Functional mapping of the primate auditory system. Science 299:568–572.

Price CJ (2000) The anatomy of language: contributions from functional neuroimaging. J Anat 197:335–359.

Rademacher J, Caviness VS, Steinmetz H, Galaburda AM (1993) Topographic variation of the human primary cortices and its relevance to brain mapping and neuroimaging studies. Cereb Cortex 3:313–329.

Rademacher J, Morosan P, Schormann T, Schleicher A, Werner C, Freund HJ, Zilles K (2001) Probabilistic mapping and volume measurement of human primary auditor cortex. NeuroImage 13:669–683.

Reale RA, Kettner RE (1986) Topography of binaural organization in primary auditory cortex of the cat: effects of changing interaural intensity. J Neurophysiol 56:663–682.

Rivier F, Clarke S (1997) Cytochrome oxidase, acetylcholinesterase, and NADPH-diaphorase staining in human supratemporal and insular cortex: evidence for multiple auditory areas. NeuroImage 6:288–304.

Robin DA, Tranel D, Damasio H (1990) Auditory perception of temporal and spectral events in patients with focal left and right cerebral lesions. Brain Lang 39:539–555.

Rutkowski RG, Wallace MN, Shackleton TM, Palmer AR (2000) Organisation of binaural interactions in the primary and dorsocaudal fields of the guinea pig auditory cortex. Hear Res 145:177–189.

Scheffler K, Bilecen D, Schmid N, Tschopp K, Seelig J (1998) Auditory cortical responses in hearing subjects and unliateral deaf patients as detected by functional magnetic resonance imaging. Cereb Cortex 8:156–163.

Scott SK, Johnsrude IS (2003) The neuroanatomical and functional organization of speech perception. Trends Neurosci 26:100–107.

Scott SK, Blank CC, Rosen S, Wise RJ (2000) Identification of a pathway for intelligible speech in the left temporal lobe. Brain 123:2400–2406.

Shapleske J, Rossell SL, Woodruff PW, David AS (1999) The planum temporale: a systematic, quantitative review of its structural, functional and clinical significance. Brain Res Rev 29:26–49.

Springer JA, Binder JR, Hammeke TA, Swanson SJ, Frost JA, Bellgowan PS, Brewer CC, Perry HM, Morris GL, Mueller WM (1999) Language dom-

inance in neurologically normal and epilepsy subjects: a functional MRI study. Brain 122:2033–2046.

Suzuki M, Kouzaki H, Ito R, Shiino A, Nishida Y, Kitano H (2002) Cortical activation patterns in functional magnetic resonance images following monaural pure tone stimulation. Neurosci Res Commun 30:197–206.

Tanaka H, Fujita N, Watanabe Y, Hirabuki N, Takanashi M, Oshiro Y, Nakamura H (2000) Effects of stimulus rate on the auditory cortex using fMRI with 'sparse' temporal sampling. NeuroReport 11:2045–2049.

Wessinger CM., VanMeter J, Tian B, Van Lare J, Pekar J, Rauschecker JP (2001) Hierarchical organization of the human auditory cortex revealed by functional magnetic resonance imaging. J Cognit Neurosci 13:1–7.

Wiegell MR, Tuch DS, Larsson HB, Wedeen VJ (2003) Automatic segmentation of thalamic nuclei from diffusion tensor magnetic resonance imaging. NeuroImage 19:391–401.

Wilson JL, Jenkinson M, de Araujo I, Kringelbach ML, Rolls ET, Jezzard P (2002) Fast, fully automated global and local magnetic field optimization for fMRI of the human brain. NeuroImage 17:967–976.

Woldorff MG, Templemann C, Fell J, Tegeler C, Gascher-Markefski B, Hinrichs H, Heinze H-J, Scheich H (1999) Lateralized auditory spatial perception and the contralaterality of cortical processing as studied with functional magnetic resonance imaging and magnetoencephalography. Hum Brain Mapp 7:49–66.

Wong PC (2002) Hemispheric specialization of linguistic pitch patterns. Brain Res Bull 59:83–95.

Woolrich MW, Ripley BD, Brady JM, Smith SM (2001) Temporal autocorrelation in univariate linear modelling of fMRI data. NeuroImage 14:1370–1386.

Yeni-Komshian GH, Benson DA (1976) Anatomical study of cerebral asymmetry in the temporal lobe of humans, chimpanzees, and rhesus monkeys. Science 192:387–389.

Zatorre RJ, Evans AC, Meyer E, Gjedde A (1992) Lateralization of phonetic and pitch discrimination in speech processing. Science 256:846–849.

Zatorre RJ, Belin P, Penhune VB (2002) Structure and function of auditory cortex: music and speech. Trends Cogn Sci 6:37–46.